

Exergetic efficiency optimization for an irreversible heat pump working on reversed Brayton cycle

YUEHONG BI^{1,2}, LINGEN CHEN^{2,*} and FENGRUI SUN²

¹Institute of Civil & Architectural Engineering, Beijing University of Technology, Beijing 100124, People's Republic of China

²Postgraduate School, Naval University of Engineering, Wuhan 430033, People's Republic of China

*Corresponding author. E-mail: lgchenna@yahoo.com; lingenchen@hotmail.com

MS received 7 December 2008; revised 18 August 2009; accepted 17 November 2009

Abstract. This paper deals with the performance analysis and optimization for irreversible heat pumps working on reversed Brayton cycle with constant-temperature heat reservoirs by taking exergetic efficiency as the optimization objective combining exergy concept with finite-time thermodynamics (FTT). Exergetic efficiency is defined as the ratio of rate of exergy output to rate of exergy input of the system. The irreversibilities considered in the system include heat resistance losses in the hot- and cold-side heat exchangers and non-isentropic losses in the compression and expansion processes. The analytical formulas of the heating load, coefficient of performance (COP) and exergetic efficiency for the heat pumps are derived. The results are compared with those obtained for the traditional heating load and coefficient of performance objectives. The influences of the pressure ratio of the compressor, the allocation of heat exchanger inventory, the temperature ratio of two reservoirs, the effectiveness of the hot- and cold-side heat exchangers and regenerator, the efficiencies of the compressor and expander, the ratio of hot-side heat reservoir temperature to ambient temperature, the total heat exchanger inventory, and the heat capacity rate of the working fluid on the exergetic efficiency of the heat pumps are analysed by numerical calculations. The results show that the exergetic efficiency optimization is an important and effective criterion for the evaluation of an irreversible heat pump working on reversed Brayton cycle.

Keywords. Exergetic efficiency; optimization; irreversible; heat pump working on reversed Brayton cycle; finite-time thermodynamics.

PACS Nos 05.70.Ln; 05.70.-a; 05.60.Cd

1. Introduction

The finite-time thermodynamics (FTT) or entropy-generation minimization (EGM) [1–18] is a powerful tool for analysing and optimizing the performance of thermodynamic processes and cycles. The results obtained for various thermodynamic cycles using FTT are closer to real device performance than those obtained using classical thermodynamics. Due to environmental damage (ozone layer, global warming) by

CFC refrigerants, the analysis for heat pump working on reversed Brayton cycle which uses air as the refrigerant and meets all criteria for a refrigerant being environmental friendly has been preferred [19–26]. Many important works about heat pumps working on reversed Brayton cycle applying FTT have been published in recent years [12,27–32]. The performance analysis and optimization for heat pump cycles were carried out by taking the heating load and the coefficient of performance (COP) as the optimization objectives [26–31]. The heating load density was also taken as the optimization objective [32].

In recent years, the research combining classical exergy concept [33–35] with FTT [1–18] is becoming increasingly important. Exergy output optimization and exergetic efficiency optimization for endoreversible cogeneration cycle [36], endoreversible and irreversible Carnot refrigeration cycles [37,38] and irreversible Brayton refrigeration cycle [39] were carried out. In this paper, exergetic efficiency optimization for an irreversible heat pump working on reversed Brayton cycle is investigated. The irreversibilities considered in the system include heat resistance losses in the hot- and cold-side heat exchangers and non-isentropic losses in the compression and expansion processes. The influences of various parameters on the characteristic of the heat pump are analysed by numerical examples. The results may help to better understand the performance of the irreversible heat pump working on reversed Brayton cycle and provide guidelines for the design of practical heat pump plants.

2. Irreversible heat pump working on reversed Brayton cycle model

The diagram of an irreversible heat pump working on reversed Brayton cycle (BCHP) and its surroundings are shown in figure 1. The following assumptions are made for this model:

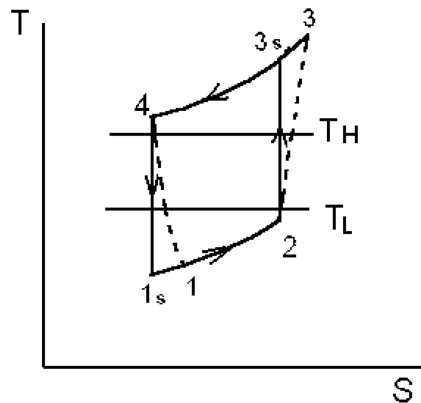


Figure 1. Temperature–entropy diagram of an irreversible heat pump working on reversed Brayton cycle with constant temperature heat reservoirs.

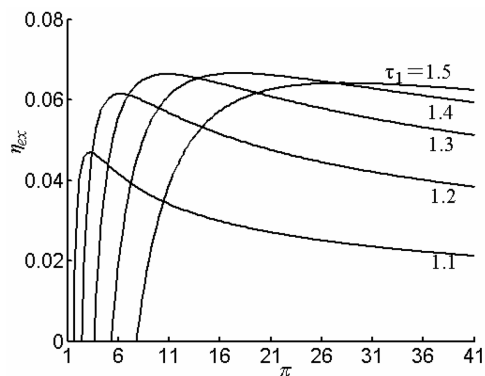


Figure 2. Effect of heat reservoir temperature ratio on the exergetic efficiency vs. pressure ratio.

Irreversible heat pump working on reversed Brayton cycle

(i) The working fluid flows through the system in a steady-state fashion. The irreversible BHP consists of two isobaric processes (1-2, 3-4) and two non-isentropic adiabatic processes (2-3, 4-1). The two adiabatic processes (2-3_s, 4-1_s) are the corresponding isentropic ones. Adiabatic accessibility of a thermodynamic state from another state is an important issue in the study of heat pumps especially the ones based on irreversible processes.

Therefore, cycle 1-2-3-4-1 is an irreversible one and 1_s-2-3_s-4-1_s is an endoreversible one. The irreversible and endoreversible cycles are distinguished by using the efficiencies of the non-isentropic compression and expansion processes. The compressor and expander efficiencies are defined as

$$\eta_c = \frac{(T_{3s} - T_2)}{(T_3 - T_2)}, \quad \eta_t = \frac{(T_4 - T_1)}{(T_4 - T_{1s})}. \quad (1)$$

For irreversible cycle, the internal irreversibility, i.e., non-isentropic losses in the compression and expansion processes are considered, $\eta_c < 1$ and $\eta_t < 1$ are satisfied. When the two adiabatic processes become reversible, the compressor and expander efficiencies are $\eta_c = \eta_t = 1$, the cycle becomes an endoreversible one (i.e. with the sole irreversibility of heat resistance) (with the loss of only heat resistance).

(ii) The heat reservoirs have infinite thermal capacitance rates. The heat sink is at temperature T_H and the heat source at T_L .

(iii) The hot- and cold-side heat exchangers are considered to be counter-flow heat exchangers, and their heat conductances (product of heat transfer coefficient and area) are U_H and U_L , respectively. The working fluid is an ideal gas having constant thermal capacitance rate (the product of mass flow rate and specific heat), C_{wf} .

According to the properties of the heat transfers between the heat reservoir and working fluid and the theory of the heat exchangers, the rate of heat transfer (Q_H) released to the heat sink, i.e., the heating load, and the rate of heat transfer (Q_L) supplied by the heat source, are, respectively, given by

$$Q_H = \frac{U_H(T_3 - T_4)}{\ln[(T_3 - T_H)/(T_4 - T_H)]} = C_{wf}E_H(T_3 - T_H), \quad (2)$$

$$Q_L = \frac{U_L(T_2 - T_1)}{\ln[(T_L - T_1)/(T_L - T_2)]} = C_{wf}E_L(T_L - T_1), \quad (3)$$

where U is the heat conductance, E is the effectiveness of the heat exchanger and N is the number of heat transfer units, and are defined as

$$E_H = 1 - \exp(-N_H), \quad E_L = 1 - \exp(-N_L), \quad (4)$$

$$N_H = \frac{U_H}{C_{wf}}, \quad N_L = \frac{U_L}{C_{wf}}. \quad (5)$$

3. Analytical relations

3.1 The heating load and the COP

The second law of thermodynamics requires $T_2T_4 = T_{1s}T_{3s}$. Combining eqs (1)–(5) gives

$$T_1 = \frac{E_H T_H \eta_c (\eta_t x^{-1} - \eta_t + 1) + E_L T_L (1 - E_H)(x + \eta_c - 1) \times (\eta_t x^{-1} - \eta_t + 1)}{\eta_c - (1 - E_H)(1 - E_L)(x + \eta_c - 1)(\eta_t x^{-1} - \eta_t + 1)}, \quad (6)$$

$$T_2 = \frac{\eta_c [E_L T_L + E_H T_H (1 - E_L)(\eta_t x^{-1} - \eta_t + 1)]}{\eta_c - (1 - E_H)(1 - E_L)(x + \eta_c - 1)(\eta_t x^{-1} - \eta_t + 1)}, \quad (7)$$

where x is the isentropic temperature ratio of the working fluid, that is, $x = T_{3s}/T_2 = (P_3/P_2)^m = \pi^m$, where π is the pressure ratio of the compressor, $m = (k - 1)/k$, and k is the ratio of specific heats. Combining eqs (2)–(7) gives the heating load (Q_H) and the COP (β) of the cycle

$$Q_H = \frac{C_{wf} E_H \{ (x + \eta_c - 1) E_L T_L - [\eta_c - (1 - E_L)(x + \eta_c - 1) \times (\eta_t x^{-1} - \eta_t + 1)] T_H \}}{\eta_c - (1 - E_H)(1 - E_L)(x + \eta_c - 1) \times (\eta_t x^{-1} - \eta_t + 1)}, \quad (8)$$

$$1 - \beta^{-1} = \frac{E_L \{ [\eta_c - (1 - E_H)(\pi^m + \eta_c - 1)(\eta_t \pi^{-m} - \eta_t + 1)] - E_H (\eta_t \pi^{-m} - \eta_t + 1) \eta_c \tau_1 \}}{E_H \{ (\pi^m + \eta_c - 1) E_L - [\eta_c - (1 - E_L)(\pi^m + \eta_c - 1) \times (\eta_t \pi^{-m} - \eta_t + 1)] \tau_1 \}}. \quad (9)$$

When $\eta_c = \eta_t = 1$ is satisfied, the two adiabatic processes become reversible, and the irreversible cycle becomes endoreversible. The heating load (Q_H) and the COP (β) of the endoreversible cycle are, respectively

$$Q_H = C_{wf} E_H E_L [T_L / (1 - \beta^{-1}) - T_H] (E_H + E_L - E_H E_L) \quad (10)$$

$$\beta = \frac{\pi^m}{\pi^m - 1}. \quad (11)$$

Equation (11) indicates that the COP of endoreversible cycle is only dependent on the pressure ratio. The dimensionless heating load \bar{Q}_H is given by

$$\begin{aligned} \bar{Q}_H &= \frac{Q_H}{C_{wf} T_H} \\ &= \frac{E_H \{ (\pi^m + \eta_c - 1) \frac{E_L}{\tau_1} - [\eta_c - (1 - E_L)(\pi^m + \eta_c - 1) \times (\eta_t \pi^{-m} - \eta_t + 1)] \}}{\eta_c - (1 - E_H)(1 - E_L)(\pi^m + \eta_c - 1)(\eta_t \pi^{-m} - \eta_t + 1)}, \end{aligned} \quad (12)$$

Irreversible heat pump working on reversed Brayton cycle

where $\tau_1 = T_H/T_L$ is the temperature ratio of the heat reservoirs. When $\eta_c = \eta_t = 1$ is satisfied, the dimensionless heating load \bar{Q}_H of the endoreversible cycle is

$$\bar{Q}_H = \frac{E_H E_L (\pi^m / \tau_1 - 1)}{(E_H + E_L - E_H E_L)}. \quad (13)$$

3.2 The exergetic efficiency

The rate of exergy input Ξ_{in} is the negative value of net work transfer rate W_{cv} that crosses the system boundary. That is,

$$\Xi_{in} = -W_{cv} = Q_H - Q_L. \quad (14)$$

The purpose of employing a heat pump system is to release heat for heating space. The rate of exergy output utilized is the negative value of exergy transfer rate accompanying heat $\sum_j (T_0/T_j - 1)Q_j$. It gives

$$\Xi_{out} = -\sum_j (1 - T_0/T_j)Q_j = \int_H (1 - T_0/T)dQ - \int_L (1 - T_0/T)dQ. \quad (15a)$$

It is also noted that the values of exergy output rates are different for equivalent heat transfer rates at various boundary temperatures. For the purposes of calculating the heat exergy, the heat reception and heat rejection are assumed to take place at T_L and T_H , respectively.

$$\Xi_{out} = (1 - T_0/T_H)Q_H - (1 - T_0/T_L)Q_L. \quad (15b)$$

From the above, the following equation is also obtained:

$$\Xi_{out} = \Xi_{in} - \Xi_d. \quad (16)$$

The exergetic efficiency is defined as the ratio of rate of exergy output to rate of exergy input

$$\eta_{ex} = \frac{\Xi_{out}}{\Xi_{in}}. \quad (17)$$

So, the exergetic efficiency is obtained as

$$\eta_{ex} = \frac{[(1 - T_0/T_H)Q_H - (1 - T_0/T_L)Q_L]}{Q_H - Q_L}. \quad (18)$$

Combining eqs (2), (3), (6), (7) and (18) gives

$$\eta_{\text{ex}} = \frac{E_L(a_1 - 1)\{\eta_c - (\eta_t \pi^{-m} - \eta_t + 1)[(1 - E_H)(\pi^m + \eta_c - 1) + \eta_c E_H \tau_1]\} - E_H(a_2 - 1)\{(\pi^m + \eta_c - 1)E_L + [(1 - E_L)(\pi^m + \eta_c - 1) \times (\eta_t \pi^{-m} - \eta_t + 1) - \eta_c] \tau_1\}}{2E_H\{(\pi^m + \eta_c - 1)E_L + [(1 - E_L)(\pi^m + \eta_c - 1) \times (\eta_t \pi^{-m} - \eta_t + 1) - \eta_c] \tau_1\} - 2E_L\{\eta_c - (\eta_t \pi^{-m} - \eta_t + 1)[(1 - E_H)(\pi^m + \eta_c - 1) + \eta_c E_H \tau_1]\}}, \quad (19)$$

where $\tau_2 = T_H/T_0$ is the ratio of the hot-side heat reservoir temperature to the ambient temperature, $a_1 = 2T_0/T_L - 1 = 2\tau_1/\tau_2 - 1$, and $a_2 = 2T_0/T_H - 1 = 2/\tau_2 - 1$. When $\eta_c = \eta_t = 1$ is satisfied, the exergetic efficiency of the endoreversible cycle is

$$\eta_{\text{ex}} = \frac{[(1 - a_2)\pi^m - (1 - a_1)]}{[2(\pi^m - 1)]}. \quad (20)$$

Equation (20) indicates that the exergetic efficiency of endoreversible cycle depends on the pressure ratio, the temperature ratio of the heat reservoirs and the ratio of the hot-side heat reservoir temperature to the ambient temperature.

4. Effects of design parameters on exergetic efficiency

Equation (16) indicates that when the temperature ratio of the heat reservoir (τ_1) and the ratio of hot-side heat reservoir temperature to ambient temperature (τ_2) are fixed, the exergetic efficiency (η_{ex}) of the irreversible heat pump working on reversed Brayton cycle is dependent on the external heat transfer irreversibility (E_H, E_L), the internal irreversibility (η_c, η_t) and the pressure ratio (π).

Figure 2 shows the effect of heat reservoir temperature ratio (τ_1) on the exergetic efficiency (η_{ex}) vs. the pressure ratio (π) for $k = 1.4$, $E_H = E_L = 0.9$, $\eta_c = \eta_t = 0.8$ and $\tau_2 = 1$. It can be seen that the curve of η_{ex} vs. π is parabolic. That is, there exists an optimum pressure ratio ($\pi_{\text{opt}, \eta_{\text{ex}}}$), which leads to a maximum exergetic efficiency ($\eta_{\text{ex max}, \pi}$). Furthermore, $\eta_{\text{ex max}, \pi}$ increases at first and then decreases with the increase of the temperature ratio of the heat reservoirs (τ_1), while the optimum pressure ratio ($\pi_{\text{opt}, \eta_{\text{ex}}}$) increases with the increase of the temperature ratio of the heat reservoirs (τ_1). The pressure ratio at which exergetic efficiency is equal to zero becomes larger when the temperature ratio of the heat reservoirs (τ_1) increases.

For comparison with figure 2, figure 3 indicates the effect of heat reservoir temperature ratio (τ_1) on the dimensionless heating load (\bar{Q}_H) vs. the pressure ratio (π). The figure illustrates that the dimensionless heating load (\bar{Q}_H) increases monotonously with increase in the pressure ratio (π), and it decreases with the increase of the temperature ratio of the heat reservoirs (τ_1).

Figure 4 shows the exergetic efficiency (η_{ex}) and the dimensionless heating load (\bar{Q}_H) vs. the COP (β). In the calculations, $k = 1.4$, $\tau_1 = 1.25$, $\tau_2 = 1$, $E_H = E_L = 0.9$ and $\eta_c = \eta_t = 0.8$ are set. It can be seen that the exergetic efficiency (η_{ex}) is an increasing function of the COP (β), and the curve of the dimensionless heating load (\bar{Q}_H) vs. the COP (β) is parabolic. Thus, when the performance optimization of the heat pump working on reversed Brayton cycle is carried out by selecting the pressure ratio, increasing the heating load inevitably

Irreversible heat pump working on reversed Brayton cycle

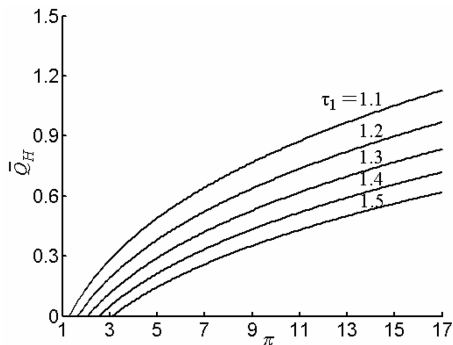


Figure 3. Effect of heat reservoir temperature ratio on the dimensionless heating load vs. pressure ratio.

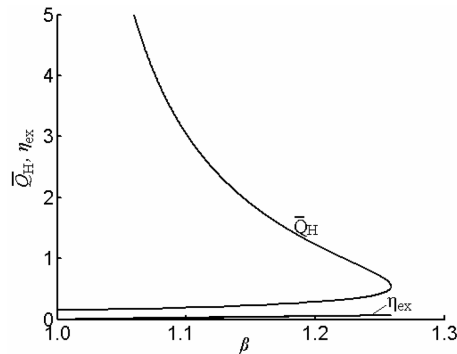


Figure 4. Exergetic efficiency and the dimensionless heating load vs. the COP.

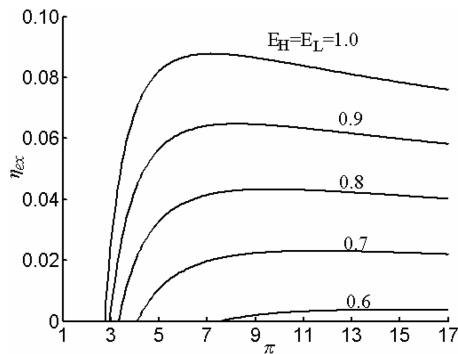


Figure 5. Effect of effectivenesses of the heat exchangers on the exergetic efficiency vs. pressure ratio.

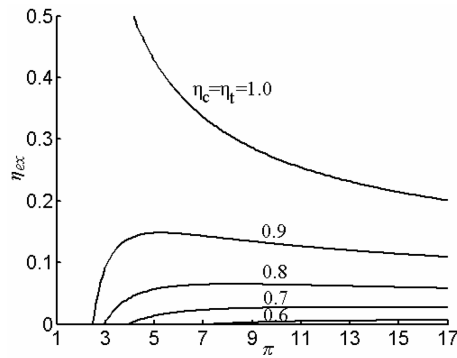


Figure 6. Effect of efficiencies of the compressor and expander on the exergetic efficiency vs. pressure ratio.

results in the decrease in the COP if \bar{Q}_H is larger than certain value, but optimizing the exergetic efficiency can simultaneously increase the COP. In this instance, the exergetic efficiency optimization objective is more practical and effective than the traditional heating load optimization objective.

Figures 5–7 show the effects of the effectivenesses of the hot- and cold-side heat exchangers (E_H and E_L), the efficiencies of the compressor and expander (η_c and η_t), and the ratio of hot-side heat reservoir temperature to ambient temperature (τ_2) on the exergetic efficiency (η_{ex}) vs. the pressure ratio (π) characteristics, respectively. They indicate that η_{ex} increases with increases of the parameters mentioned above, respectively. The result shown in figure 6 with $\eta_c = \eta_t = 1$ is that of an endoreversible cycle.

Figures 8 and 9 show the effects of the effectivenesses of the hot- and cold-side heat exchangers (E_H and E_L), and the efficiencies of the compressor and expander (η_c and η_t) on the optimum pressure ratio ($\pi_{opt, \eta_{ex}}$) vs. heat reservoir temperature

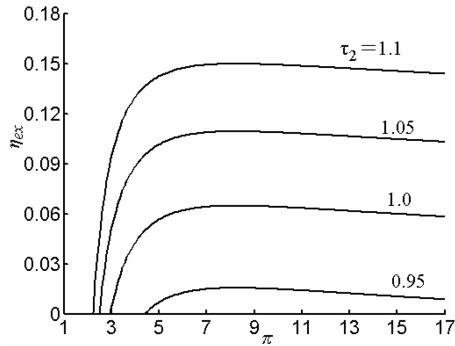


Figure 7. Effect of the ratio of hot-side heat reservoir temperature to ambient temperature on the exergetic efficiency vs. pressure ratio.

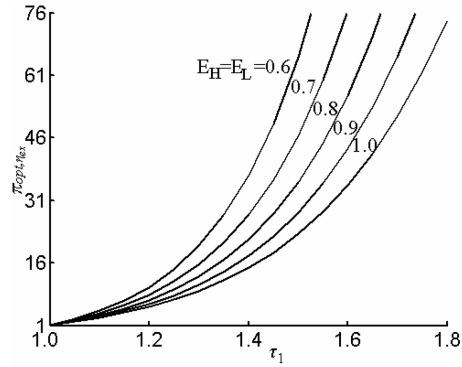


Figure 8. Effect of effectivenesses of the heat exchangers on the optimum pressure ratio vs. heat reservoir temperature ratio.

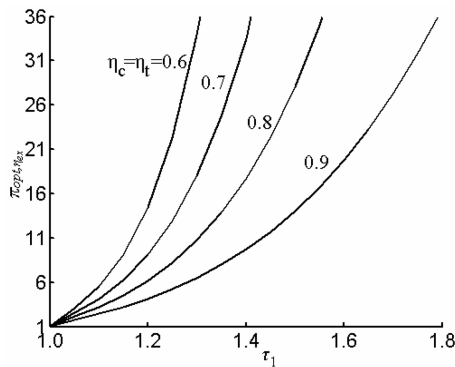


Figure 9. Effect of efficiencies of the compressor and expander on the optimum pressure ratio vs. heat reservoir temperature ratio.

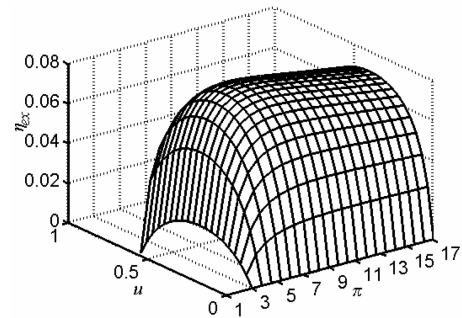


Figure 10. Comprehensive relationships among exergetic efficiency, distribution of heat conductance and pressure ratio.

ratio (τ_1), respectively. Those figures indicate that the optimum pressure ratio ($\pi_{opt, \eta_{ex}}$) decreases with increase of the parameters mentioned above, respectively.

5. Optimal distribution of heat exchange inventory

For the fixed total heat exchanger inventory U_T , that is, when $U_H + U_L = U_T$, defining the distribution of heat conductance $u = U_L/U_T$ leads to

$$U_L = uU_T, \quad U_H = (1 - u)U_T. \quad (21)$$

Figure 10 shows the corresponding three-dimensional diagram among η_{ex} , u and π . In the calculations, $k = 1.4$, $C_{wf} = 0.8 \text{ kW/K}$, $U_T = 5 \text{ kW/K}$, $\eta_c = \eta_t = 0.8$,

Irreversible heat pump working on reversed Brayton cycle

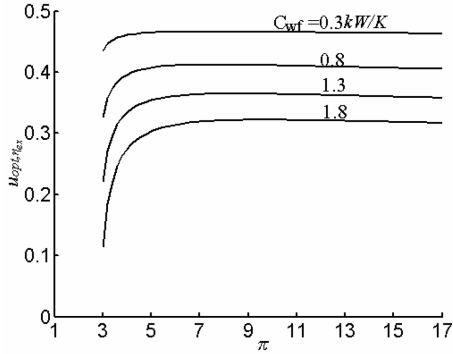


Figure 11. Effect of thermal capacity rate of the working fluid on the optimum distribution of heat conductance vs. pressure ratio.

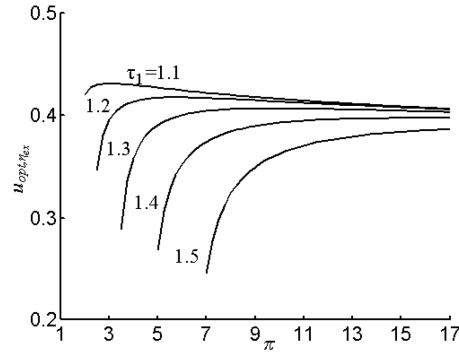


Figure 12. Effect of heat reservoir temperature ratio on the optimum distribution of heat conductance vs. pressure ratio.

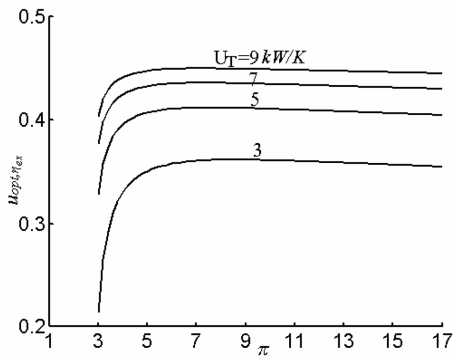


Figure 13. Effect of total heat exchanger inventory on the optimum distribution of heat conductance vs. pressure ratio.

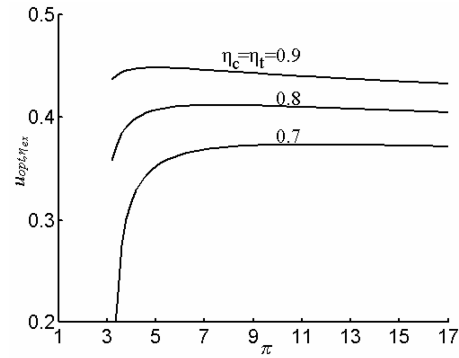


Figure 14. Effect of efficiencies of the compressor and expander on the optimum distribution of heat conductance vs. pressure ratio.

$\tau_1 = 1.25$ and $\tau_2 = 1$ are set. It indicates that the curve of η_{ex} vs. u is also parabolic. There exists an optimum allocation ($u_{opt,\eta_{ex}}$) of heat conductance corresponding to maximum exergetic efficiency ($\eta_{ex\ max,u}$) for a fixed pressure ratio. Therefore, there exist an optimum distribution ($u_{opt,\eta_{ex}}$) of heat conductance and an optimum pressure ratio ($\pi_{opt,\eta_{ex}}$), which lead to a double maximum exergetic efficiency ($\eta_{ex\ max,max}$).

Figure 11 shows the influence of thermal capacity rate of the working fluid (C_{wf}) on the optimum distribution ($u_{opt,\eta_{ex}}$) of heat conductance vs. pressure ratio (π) for $k = 1.4$, $U_T = 5$ kW/K, $\eta_c = \eta_t = 0.8$, $\tau_1 = 1.25$ and $\tau_2 = 1$. Figure 12 shows the influence of the heat reservoir temperature ratio (τ_1) on the optimum distribution ($u_{opt,\eta_{ex}}$) of heat conductance vs. pressure ratio for $k = 1.4$, $U_T = 5$ kW/K, $C_{wf} = 0.8$ kW/K, $\eta_c = \eta_t = 0.8$ and $\tau_2 = 1$. Figure 13 shows the

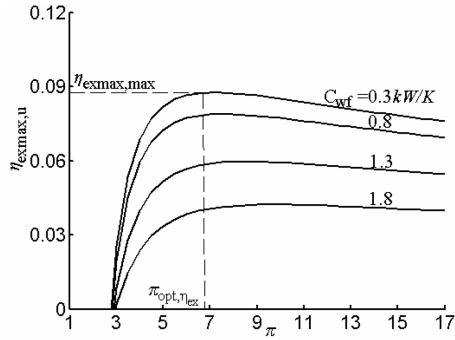


Figure 15. Effect of thermal capacity rate of the working fluid on the maximum exergetic efficiency vs. pressure ratio.

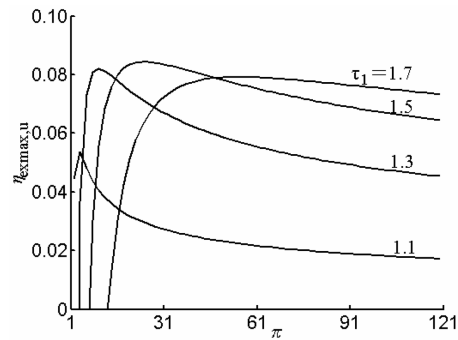


Figure 16. Effect of heat reservoir temperature ratio on the maximum exergetic efficiency vs. pressure ratio.

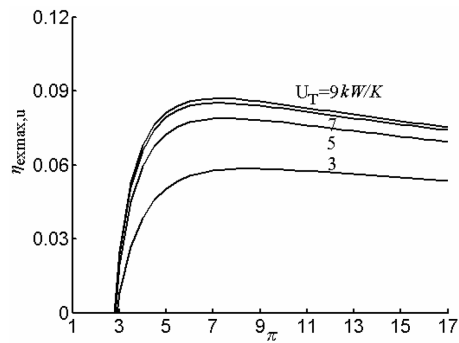


Figure 17. Effect of total heat exchanger inventory on the maximum exergetic efficiency vs. pressure ratio.

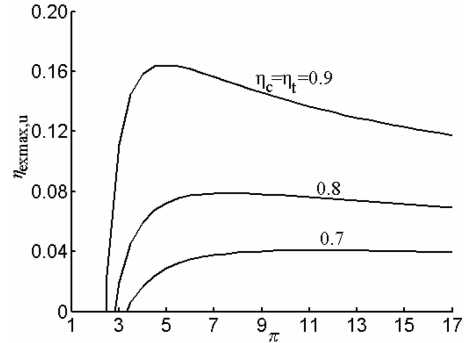


Figure 18. Effect of efficiencies of the compressor and expander on the maximum exergetic efficiency vs. pressure ratio.

influence of the total heat exchanger inventory (U_T) on the optimum distribution ($u_{opt,\eta_{ex}}$) of heat conductance vs. pressure ratio for $k = 1.4$, $\tau_1 = 1.25$, $C_{wf} = 0.8$ kW/K, $\tau_2 = 1$ and $\eta_c = \eta_t = 0.8$. Figure 14 shows the influences of efficiencies of the compressor and expander (η_c and η_t) on the optimum distribution ($u_{opt,\eta_{ex}}$) of heat conductance vs. pressure ratio for $k = 1.4$, $\tau_1 = 1.25$, $\tau_2 = 1$, $C_{wf} = 0.8$ kW/K and $U_T = 5$ kW/K.

The numerical calculations show that $u_{opt,\eta_{ex}}$ is an increasing function of π , and $u_{opt,\eta_{ex}}$ increases very quickly when π is smaller, while it almost is unchangeable when π gets larger. It decreases with the increase of C_{wf} or τ_1 , while it increases with the increase of U_T or η_c and η_t , and it increases less if U_T gets larger. It is always less than 0.5.

The influence of thermal capacity rate of the working fluid (C_{wf}) on the maximum exergetic efficiency ($\eta_{ex,max,u}$) vs. the pressure ratio (π) for $k = 1.4$, $U_T = 5$ kW/K, $\eta_c = \eta_t = 0.8$, $\tau_1 = 1.25$ and $\tau_2 = 1$ are shown in figure 15. The influence of the

heat reservoir temperature ratio (τ_1) on the maximum exergetic efficiency vs. the pressure ratio (π) for $k = 1.4$, $U_T = 5$ kW/K, $C_{wf} = 0.8$ kW/K, $\eta_c = \eta_t = 0.8$ and $\tau_2 = 1$ are shown in figure 16. The influence of the total heat exchanger inventory (U_T) on the maximum exergetic efficiency vs. the pressure ratio (π) for $k = 1.4$, $\tau_1 = 1.25$, $C_{wf} = 0.8$ kW/K, $\tau_2 = 1$ and $\eta_c = \eta_t = 0.8$ are shown in figure 17. The influences of efficiencies of the compressor and expander (η_c and η_t) on the maximum exergetic efficiency vs. the pressure ratio (π) for $k = 1.4$, $\tau_1 = 1.25$, $\tau_2 = 1$, $C_{wf} = 0.8$ kW/K and $U_T = 5$ kW/K are shown in figure 18.

The numerical calculations show that $\eta_{ex\ max,u}$ decreases with the increase of C_{wf} , while it increases with the increase of U_T or η_c and η_t , and it increases less if U_T gets larger. $\eta_{ex\ max,max}$ increases at first and then decreases with the increase of τ_1 .

6. Conclusion

Optimization of exergetic efficiency for an irreversible heat pump working on reversed Brayton cycle was performed in this paper. The expression of the exergetic efficiency was deduced based on the theoretical model of the heat pump. Then, the influences of the pressure ratio of the compressor, the allocation of heat exchanger inventory, the temperature ratio of the two reservoirs, the effectivenesses of the hot- and cold-side heat exchangers, the efficiencies of the compressor and expander, the ratio of hot-side heat reservoir temperature to ambient temperature, the total heat exchanger inventory and the heat capacity rate of the working fluid on the exergetic efficiency of the heat pump were investigated by detailed numerical examples. Moreover, performance comparisons between exergetic efficiency optimization objective and traditional heating load optimization objective were carried out.

In general, there exists an optimum pressure ratio ($\pi_{opt,\eta_{ex}}$) corresponding to an optimum exergetic efficiency ($\eta_{ex\ max,\pi}$) and when pressure ratio is chosen as a fixed value or just the optimum value there exists an optimum distribution ($u_{opt,\eta_{ex}}$) of heat conductance corresponding to another optimum exergetic efficiency ($\eta_{ex\ max,u}$). Therefore, there exists a double maximum value ($\eta_{ex\ max,max}$) for the exergetic efficiency. The results show that the exergetic efficiency optimization objective is more practical and effective than the traditional heating load optimization objective.

Acknowledgements

This paper is supported by Scientific Research Common Program of Beijing Municipal Commission of Education (Project No. KM200710005034), China Postdoctoral Science Foundation (Project No. CPSF20060400837), Beijing Municipality Key Lab of Heating, Gas Supply, Ventilating and Air Conditioning Engineering and Program for New Century Excellent Talents in University of P. R. China (Project No. NCET-04-1006). The authors wish to thank the reviewers for their careful, unbiased and constructive suggestions, which led to this revised manuscript.

References

- [1] B Andresen, R S Berry, M J Ondrechen and P Salamon, *Acc. Chem. Res.* **17(8)**, 266 (1984)
- [2] D C Agrawal and V J Menon, *Eur. J. Phys.* **11(5)**, 305 (1990)
- [3] D C Agrawal and V J Menon, *J. Appl. Phys.* **74(4)**, 2153 (1993)
- [4] D C Agrawal, J M Gordon and M Huleihil, *Indian J. Engng. Mater. Sci.* 1 (Aug.) 195–198 (1994)
- [5] A Bejan, *Entropy generation minimization* (CRC Press, Boca Raton, FL, 1996)
- [6] M Feidt, *Thermodynamique et Optimisation Energetique des Systems et Procèdes*, 2nd edn (Technique et Documentation, Lavoisier, Paris, 1996) (in French)
- [7] R S Berry, V A Kazakov, S Sieniutycz, Z Szwast and A M Tsirlin, *Thermodynamic optimization of finite time processes* (Wiley, Chichester, 1999)
- [8] L Chen, C Wu and F Sun, *J. Non-Equilib. Thermodyn.* **24(3)**, 327 (1999)
- [9] A Durmayaz, O S Sogut, B Sahin and H Yavuz, *Prog. Energy & Combust. Sci.* **30(2)**, 175 (2004)
- [10] L Chen and F Sun, *Advances in finite time thermodynamics: Analysis and optimization* (Nova Science Publishers, New York, 2004)
- [11] S K Tyagi, G Lin, S C Kaushik and J Chen, *Int. J. Refrig.* **27(6)**, 924 (2004)
- [12] L Chen, *Finite-time thermodynamic analysis of irreversible processes and cycles* (Higher Education Press, Beijing, 2005)
- [13] S K Tyagi, J Chen and S C Kaushik, *Int. J. Ambient Energy* **26(3)**, 155 (2005)
- [14] S K Tyagi, G M Chen, Q Wang and S C Kaushik, *Int. J. Thermal Sci.* **45(8)**, 829 (2006)
- [15] S K Tyagi, G M Chen, Q Wang and S C Kaushik, *Int. J. Refrig.* **29(7)**, 1167 (2006)
- [16] S K Tyagi, S W Wang, H Chandra, G M Chen, Q Wang and C Wu, *Int. J. Exergy* **4(1)**, 98 (2007)
- [17] S Bhattacharyya and J Sarkar, *Energy Convers. Manage.* **48(3)**, 803 (2007)
- [18] B H Li, Y R Zhao and J C Chen, *Pramana – J. Phys.* **70(5)**, 779 (2008)
- [19] J T Dieckmann, A J Erickson, A C Harvey and W M Toscano, *Research and development of an air-cycle heat pump water heater*, DOE Final Report, 1979, ORNL/Sub-7226/1: 1-341
- [20] F Sisto, *ASME Trans. J. Engng. Power* **101(4)**, 162 (1979)
- [21] J L Kovach, Utilization of the Brayton cycle heat pump for solvent recovery, *The USDOE Industrial Solvent Recycling Conference* (Charlotte, NC, 1990) NUCON286: 1-8
- [22] G Angelino and C Invernizzi, *Int. J. Refrig.* **18(4)**, 272 (1995)
- [23] M A Heikkinen, M J Lampinen and M Tamasy-Bano, *Heat Recovery Systems and Combined Heat and Power* **13(2)**, 123 (1993)
- [24] J S Fleming, B J C Van der Wekken, J A McGovern and R J M Van Gerwen, *Int. J. Energy Res.* **22(5)**, 463 (1998)
- [25] J S Fleming, L Li and B J C Van der Wekken, *Int. J. Energy Res.* **22(7)**, 639 (1998)
- [26] J E Braun, P K Bansal and E A Groll, *Int. J. Refrig.* **25(7)**, 954 (2002)
- [27] C Wu, L Chen and F Sun, *Energy Convers. Manage.* **39(5/6)**, 445 (1998)
- [28] L Chen, N Ni, C Wu and F Sun, *Int. J. Pow. Energy Systems* **21(2)**, 105 (2001)
- [29] N Ni, L Chen, C Wu and F Sun, *Energy Convers. Manage.* **40(4)**, 393 (1999)
- [30] L Chen, N Ni, F Sun and C Wu, *Int. J. Power and Energy Systems* **19(3)**, 231 (1999)
- [31] L Chen, N Ni, C Wu and F Sun, *Int. J. Energy Research* **23(12)**, 1039 (1999)
- [32] Y Bi, L Chen and F Sun, *Appl. Energy* **85(7)**, 607 (2008)

Irreversible heat pump working on reversed Brayton cycle

- [33] M J Moran, *Availability analysis: A guide to efficient energy use* (ASME Press, New York, 1989)
- [34] T J Kotas, *The exergy method of thermal plant analysis* (Krieger, Melbourne, FL, 1995)
- [35] A Bejan, G Tsatsaronis and M Moran, *Thermal design & optimization* (Wiley, New York, 1996)
- [36] B Sahin, A Kodal, I Ekmekci and T Yilmaz, *Energy, The Int. J.* **22(6)**, 551 (1997)
- [37] Y F Su and C K Chen, *Proc. IMechE Part C, J. Mech. Engng. Sci.* **220(8)**, 1179 (2006)
- [38] Y F Su and C K Chen, *Proc. IMechE Part A, Power Energy* **221(1)**, 11 (2007)
- [39] C K Chen and Y F Su, *Int. J. Thermal Sci.* **44(3)**, 303 (2005)